Frequency-Multiplexed Storage and Distribution of Narrowband Telecom Photon Pairs over a 10-km Fiber Link with Long-Term System Stability

Ko Ito,[1] Takeshi Kondo,[1] Kyoko Mannami,[1] Kazuya Niizeki,[1,2] Daisuke Yoshida,[1,2] Kohei Minaguchi,[1] Mingyang Zheng,[3] Xiuping Xie,[3] Feng-Lei Hong,[1] and Tomoyuki Horikiri[1,*]

[1] *Department of Physics, Graduate School of Engineering Science, Yokohama National University, Yokohama 240-8501, Japan*

[2] *LQUOM Inc., Yokohama 240-8501, Japan*

[3] *Jinan Institute of Quantum Technology, Jinan 250101 Shandong, China*

(Received 13 June 2022; revised 13 November 2022; accepted 27 January 2023; published 27 February 2023)

The ability to transmit quantum states over long distances is a fundamental requirement of the quantum internet and is reliant upon quantum repeaters. Quantum repeaters involve entangled photon sources that emit and deliver photonic entangled states at high rates and quantum memories that can temporarily store quantum states. Improvement of the entanglement distribution rate is essential for quantum repeaters, and multiplexing is expected to be a breakthrough. However, limited studies exist on multiplexed photon sources and their coupling with a multiplexed quantum memory. Here, we demonstrate the storing of a frequency-multiplexed two-photon source at telecommunication wavelengths in a quantum memory accepting visible wavelengths via wavelength conversion after 10-km distribution. To achieve this, quantum systems are connected via wavelength conversion with a frequency-stabilization system and a noise-reduction system. The developed system is stably operated for more than 42 h. Therefore, it can be applied to quantum repeater systems comprising various physical systems requiring long-term system stability.

DOI: 10.1103/PhysRevApplied.19.024070

I. INTRODUCTION

The quantum internet has the potential to be used in various applications, such as distributed quantum computation, cloud quantum computing [1], world clocks [2], and ultralong baseline interferometry [3]. In the quantum internet system, quantum repeaters are indispensable for sharing the entanglement of the quantum states (qubits) between adjacent repeater nodes to realize long-distance quantum communication. Quantum repeaters can be implemented in either an optical-fiber-based or a satellite-based [4] quantum communication system. Furthermore, a quantum internet using hybrid quantum communication between satellites and optical fibers is coming to fruition [5–8].

Quantum memory, which stores a quantum state for later retrieval, is a key component of the quantum repeater. Various materials working at different wavelengths are studied for quantum memory applications [9–18]. Using wavelength conversion as an intermediate step [17–20], the diversity of a network consisting of various materials can be acquired. Atomic frequency comb (AFC) [21] quantum memories based on rare-earth-doped materials are promising for multiplexed quantum communication and are essential for improving the entanglement generation rate of quantum communication [13,14]. Rare-earth-doped materials have gained considerable attention owing to the high coherence of their donors and their multiplicity by controlling the inhomogeneous width. The AFC method accepts single photons with collective donor ions, thus exhibiting high absorption and storage efficiency and enabling a high retrieval efficiency through rephasing. Among these, Pr^{3+}:Y_2SiO_5 (Pr:YSO) has demonstrated a relatively long coherence time, high multimode capacity, and high efficiency [13,22]. The AFC and memory transition wavelength of this material is approximately 606 nm; therefore, the transmitted telecommunication-wavelength photons need to be wavelength converted before being stored in the memory. This wavelength conversion can be realized based on sum-frequency generation (SFG): the frequency of the memory photon (606 nm) is the sum of the telecom photon (1.5 μm) and a wavelength-conversion pump laser (1.0 μm). Owing to the narrow bandwidth of the AFC, the frequency of the photons produced by SFG must be stabilized at the AFC frequency. Therefore, all the components, including telecom entangled-photon sources and wavelength-conversion pump lasers, must also be stabilized in addition to the quantum memory control lasers for AFC generation, which is the reference for these lasers.

*horikiri-tomoyuki-bh@ynu.ac.jp

A typical quantum repeater node has at least two quantum memories and, if necessary, after both quantum memories are loaded, photons are regenerated for quantum entanglement swapping [23]. Indistinguishability is required for successful entanglement swapping. The spectra (center frequency and linewidth) and the timing of incidence on the Bell state measurement (BSM) for swapping must be matched. For example, because the wavelength-conversion pump laser and the quantum memory control laser can be the same for the two memories used in the intranode swapping operation, the problem of spectral quantum interference between the retrieved photons from the two quantum memories can be addressed. Furthermore, by sending a laser (telecommunication-wavelength laser in the case of optical fiber transmission) that is stabilized with respect to the frequency of an optical frequency comb in one node, which is the frequency reference, frequency coordination between several repeaters is possible. Using this scheme, a multinode quantum repeater through entanglement swapping between remote quantum devices can be developed if frequency matching between the elements [24] is stable over time.

To establish a system that can perform entanglement swapping operations at quantum repeater nodes, it is necessary to combine remote quantum devices, that is, a frequency-multiplexed telecom photon source and a frequency-multiplexed quantum memory. Photons emitted from a frequency-multiplexed telecom photon source will need to be sent through a quantum communication channel consisting of a long optical fiber, wavelength converted, and stored in a frequency-multiplexed quantum memory. Until now, there has been no example of coupling two telecommunication-wavelength photons into a frequency-multiplexed memory through wavelength conversion after long-optical-fiber transmission. This can be attributed to the difficulty of implementing wavelength conversion with a high signal-to-noise ratio (SNR) under low photon rates after long-distance transmission, as well as the difficulty of frequency coordination between systems.

Here, we place an optical frequency comb as an optical frequency reference in the repeater node to enable the frequency tuning of the involved telecommunication-wavelength photons, wavelength-conversion pump laser, and quantum memory control laser. We also introduce a noise-reduction system to obtain a high SNR for the wavelength-conversion system. Using these systems, we observe signals by storing and retrieving photons from a narrow-linewidth two-photon source [13,25,26] in a fixed-time quantum memory following fiber transmission over 10 km. Because various physical systems can be used in the physical layer that constitutes the quantum internet, it is highly likely that the system will be a wavelength-conversion-mediated system for quantum communication in both satellites and optical fibers. This study is a significant step in that direction.

II. RESULTS

A. Experimental setup

In this section, we describe the overall setup of the experiment, as illustrated in Fig. 1. The experiment can be divided into the following parts: a telecom two-photon source [two-photon comb (TPC) [25]], wavelength conversion, quantum memory, noise-reduction system, and an additional frequency-stabilization system for the highly efficient coupling of the TPC and the quantum memory. In the following paragraphs, we describe each component.

The TPC consists of a periodically poled lithium niobate (PPLN) chip for generating two photons through degenerate spontaneous parametric downconversion (SPDC) and its surrounding cavity. The wavelength of an external-cavity diode laser (ECDL) at 1514 nm is converted to 757 nm through second-harmonic generation (SHG) and used as the pump laser for SPDC. The generated photon pair has a cluster width [26] of approximately 500 GHz, a linewidth of 7.1 MHz in the 1514-nm region, and a free spectral range (FSR) of 117.2 MHz.

A Pr:YSO crystal with a doping ratio of 0.05% is used for the quantum memory. The crystal is placed inside a cryostat (4 K) and has an inhomogeneous broadening of approximately 10 GHz, as depicted in Fig. 2(a). Moreover, a transparent region (pit) is created in the crystal, where an AFC (comb-shaped absorption lines) is created for photon storage and retrieval. The frequency and timing of the quantum memory control laser (606 nm), which is generated through the SHG of an ECDL at 1212 nm, are adjusted by the rf signal applied to the acousto-optic modulator (AOM) installed in the path. Initially, a small absorption region is formed by sweeping around the frequency of the $1/2g$-$1/2e$ transition of $^3H_4(0)$-$^1D_2(0)$, as depicted in Fig. 2(a), in the range of ± 9 MHz. Next, a sharp peak is formed in the transparent region by injecting a single-frequency light with a frequency of the $5/2g$-$5/2e$ transition into the crystal (this process is referred to as "burn back" [22]). The AFC is formed by repeating this process at the peak spacing of each comb (1.15 MHz in this experiment). The reference frequency in the region where this AFC is generated [ν_{AFC}, the zero point in the inset of Fig. 2(b)] is the quantum memory control laser frequency, ν_{QM}, with a constant offset applied by an AOM ($f_{\mathrm{QMpumpAOM}} = 164.3$ MHz). Frequency matching between the TPC and AFC is performed as follows: the TPC laser (1514 nm) is locked to an optical frequency comb, which is a frequency reference in this study that synchronizes with the global-positioning-system signals (GPS comb). The frequency of the quantum memory control laser is also locked to the GPS comb. Therefore, when the TPC laser is converted to 606 nm through wavelength conversion, a beat measurement is made, with the quantum memory control laser responsible for AFC generation, and feedback is applied to the wavelength-conversion laser

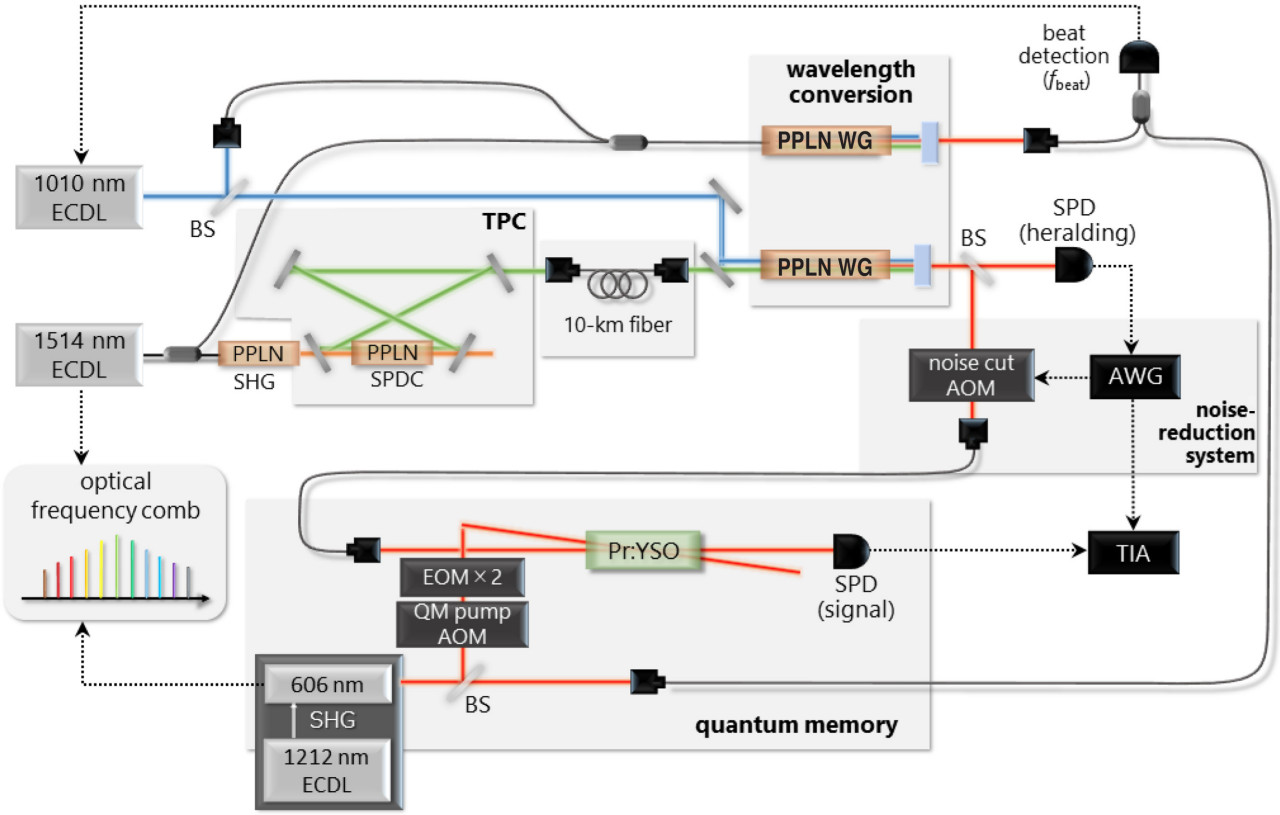

FIG. 1. Schematic of the experimental setup. Experiment comprises a two-photon comb, quantum memory, wavelength-conversion system, noise-reduction system, and frequency-stabilization system. SHG light (757 nm) from the TPC pump laser (1514 nm) causes SPDC inside the cavity at a pump power of 25 mW, generating a degenerate photon pair (1514 nm). After transmission over a 10-km-length optical fiber, the pair is converted into a quantum memory wavelength (606 nm) by SFG using a PPLN waveguide (WG). Wavelength-converted photons are split into two using a BS, and one side is detected by a SPD and used as a heralding photon. Other side is stored in quantum memory after transmission through the AOM used in the noise-reduction system, and retrieved photons are detected by a SPD. Time difference between detection on the heralding side and detection after the quantum memory is measured by a TIA. Frequency of all lasers and the TPC cavity is locked to the appropriate frequency by the frequency-stabilization system. AWG: arbitrary waveform generator.

frequency to keep the beat frequency constant (further details are provided in Sec. II B).

In this study, we also perform the frequency multiplexing of quantum memory using two electro-optic modulators (EOMs) after transmitting the light through an AOM [27]. We apply a signal of frequency ν_{FSR} (117.2 MHz), corresponding to the FSR of the TPC to the first EOM, and a signal of $5\nu_{\mathrm{FSR}}$ (586.0 MHz) to the second EOM. By adjusting the amplitude of the rf signal applied to the EOMs, 0-, $\pm$1-, and $\pm$2-order peaks are formed for each EOM, resulting in the generation of AFCs for 25 frequency modes. Figure 2(b) depicts the generated AFCs. In this study, the optical power of the quantum memory control laser is 2.3 mW.

Owing to the gap between the telecommunication-wavelength photon (1514 nm) generated by the TPC and the wavelength of the Pr:YSO quantum memory (606 nm), the photon from the TPC cannot be directly stored in the quantum memory. Therefore, we convert the telecommunication wavelength to the quantum memory wavelength (606 nm) by performing SFG using a wavelength-conversion pump laser (1010 nm) in a PPLN waveguide after the long-optical-fiber transmission of photons generated in the TPC. Following wavelength conversion, only photons with wavelengths of approximately 606 nm are extracted using two bandpass filters and two dichroic mirrors. This experiment is performed using a wavelength-conversion pump laser with a power of 140 mW and a quantum wavelength conversion efficiency of 55.8%. Limited by the phase-matching bandwidth of the PPLN waveguide, the full width at half maximum bandwidth of this wavelength-conversion system is approximately 40 GHz. The wavelength-converted photon pair is split equally by a beam splitter (BS), and one side is detected as a heralding photon by a single-photon detector (SPD). The other side is detected by a SPD after a single photon from the TPC has been stored and retrieved by the frequency-multiplexed quantum memory. The time

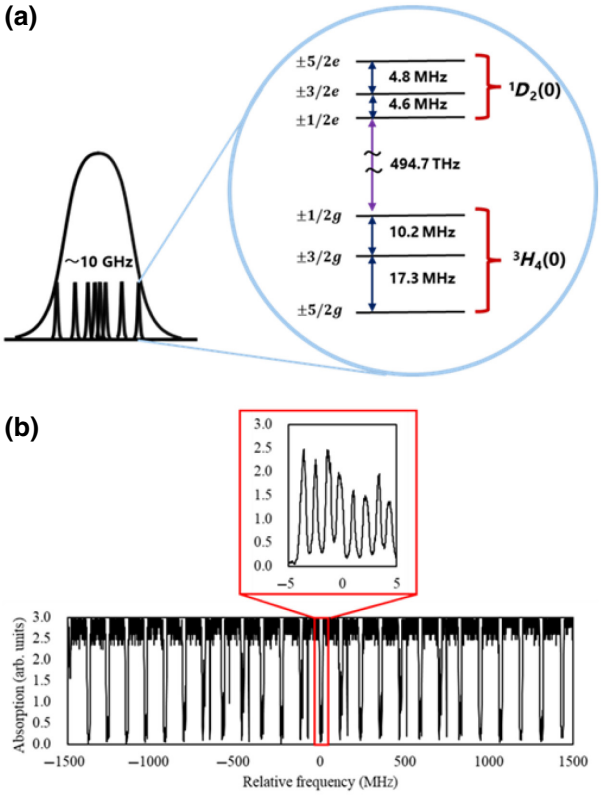

FIG. 2. Quantum memory. (a) Inhomogeneous broadening of Pr:YSO (left) and energy diagram (right). (b) This panel shows the entire 25-frequency-mode quantum memory; enlarged panel shows a magnified view of one of the frequency modes.

difference between the detection of the heralding photon and the other photon is measured using a time-interval analyzer (TIA).

B. Frequency-stabilization system

To couple wavelength-converted photons with quantum memory, it is necessary to precisely match the wavelength of the wavelength-converted photons with that of the quantum memory control laser. We achieve the desired frequency matching by developing a wavelength-conversion system for monitoring, which is different from that used for the photons. This is described as follows (see also Fig. 3). The frequencies of the TPC pump laser at approximately 1514 nm (ν_{photon}) and the master of the quantum memory control laser at approximately 1212 nm (ν_{QMmaster}) are offset locked using a delay line [24,28–30] into an optical frequency comb that synchronizes with the GPS comb. Furthermore, the resonant frequency of the TPC cavity is locked using the Pound-Drever-Hall method with a TPC pump laser [25]. The temperature of the PPLN is well stabilized within about 1 mK. In general, the resonant frequency of the TPC cavity is well locked to the TPC pump laser. A wavelength-conversion system is developed for monitoring, and feedback is returned to the wavelength-conversion pump laser by offset locking, such that the frequency of the beat signal between the 606-nm laser light for monitoring (ν_{monitor}) and the frequency of the quantum memory control laser ($\nu_{\mathrm{QM}} = 2\nu_{\mathrm{QMmaster}}$) become constant. (The detailed scheme is described in the caption of Fig. 3.)

Figure 4 presents the experimental results of the relative frequency locking. The drift of the beat frequency between ν_{QM} and ν_{monitor} for monitoring is illustrated. The frequency drift is suppressed within 5 kHz over 12 h, which is sufficient for accurate frequency matching between the wavelength-converted photons and AFCs.

C. Noise-reduction system

In this study, noise mainly originates from the strong wavelength-conversion pump laser [31–33]. The TPC photons retrieved from the quantum memory are buried in the noise without a noise-reduction system; therefore, we separate the retrieved photons from the noise through an installed noise-reduction system [34]. The noise originating from the wavelength-conversion pump laser is removed by a fast shutter consisting of an AOM. Figure 5 depicts the timescale of the entire experiment. The cycle is repeated throughout the experiment. During the photon transmission time, the AOM shutter placed after the wavelength-conversion system is operated as follows. In particular, we close the AOM shutter based on the timing of the arrival of the heralding photons to the SPD. By shuttering the light after wavelength conversion using the time difference until the photons are generated as echoes, we can separate the signal photons in the quantum memory from the noise originating from the continuously operating strong wavelength-conversion pump laser. The combination of AFC and time filtering results in filtering in the frequency domain as well, because time filtering detects only retrieved photons that are absorbed and retrieved by the AFC.

Noise originates mainly from the wavelength-conversion pumping laser. The pump laser (with a wavelength of approximately 1 μm) produces significant noise at the telecommunication wavelength owing to SPDC and Raman scattering inside the nonlinear medium when visible signal photons are converted into telecommunication wavelengths through difference frequency generation [35]. In contrast, in our case, the SFG is used for converting the telecom signal photons into visible light; the pump laser at approximately 1 μm generates the same noise at the telecommunication wavelength. This noise is also upconverted to the quantum memory wavelength in the wavelength-conversion device, causing the noise in the visible quantum memory wavelength to be less than the originally generated telecommunication-wavelength noise.

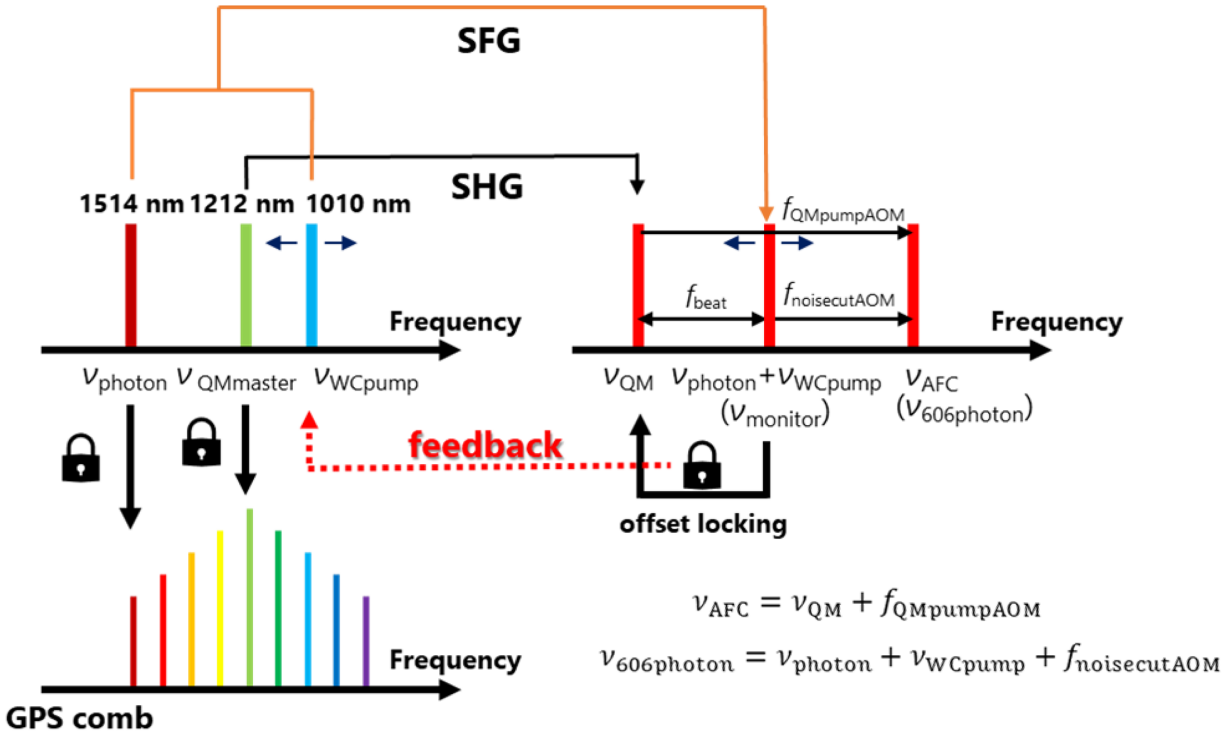

FIG. 3. Frequency-locking diagram. First, the TPC pump laser (1514 nm) and the master of the quantum memory control laser (1212 nm) are offset locked to the GPS comb. Thereafter, the wavelength-converted light for monitoring is offset locked to the quantum memory control laser (606 nm). Offset locking is achieved through feedback to the wavelength-conversion pump laser (1010 nm) for obtaining the frequency matching of telecom TPC photons with the AFC quantum memory. Because the photon before entering the quantum memory is a wavelength-converted photon generated from the TPC and passed through the noise-cutting AOM (which is discussed later) of modulation frequency ($f_{noisecutAOM}$), its frequency ($\nu_{606photon}$) is expressed as follows: $\nu_{606photon} = \nu_{monitor} + f_{noisecutAOM}$, where ν_{WCpump} is the frequency of the wavelength-conversion pump laser. Conversely, because quantum memory is generated by modulating the quantum memory control laser with an AOM (modulation frequency, $f_{QMpumpAOM}$), the frequency at which the atomic frequency comb structure (ν_{AFC}) is actually created is expressed as follows: $\nu_{AFC} = \nu_{QM} + f_{QMpumpAOM} = 2\nu_{QMmaster} + f_{QMpumpAOM}$. Because the 606-nm light for monitoring is offset locked at frequency f_{beat} to the quantum memory control laser, we obtain the following expression: . Therefore, we obtain by adjusting the frequency of ν_{WCpump} using the feedback information (f_{beat}), so that $\nu_{606photon} = \nu_{AFC}$ and relative frequency matching is achieved. In the experiment, the values of $f_{QMpumpAOM}$, f_{beat}, and $f_{noisecutAOM}$ are set as 164.3, 83.4, and 80.9 MHz, respectively.

In our case, with a phase-matched bandwidth of approximately 40 GHz, and including the wavelength-conversion efficiency (<1), the noise is approximately 40 kcps at a pump power of 140 mW. Furthermore, Fig. 6 indicates that the noise can be reduced by 2 orders of magnitude with a noise-filtering system.

D. Experimental results

Figure 6 presents the experimental results of the time difference between the heralding photon and the photon retrieved from the quantum memory measured using the TIA. The AFC is created for 25 frequency modes. TPC photons are transmitted over a 10-km optical fiber. The time resolution of the TIA is 0.128 ns, and the measurement time is 12 h. The peaks on the left side represent the transmitted photons outside the inhomogeneous broadening of Pr:YSO owing to the fact that, while the bandwidth of the wavelength conversion is approximately 40 GHz, the inhomogeneous broadening width of Pr:YSO used in this study is approximately 10 GHz. Therefore, some of the wavelength-converted photons are transmitted outside the inhomogeneous broadening. The peaks on the right side represent the photons regenerated from the AFC. Defining S as the total number of counts including noise and N as the number of noise counts, the SNR can be expressed as $\mathrm{SNR} = (S - N)/N$. The signal count S at the peak is 74 counts and the SNR is 1.4. From this result, small peaks are observed at approximately 150 ns, which is caused by the slow light effect. The slow light effect [36,37] is caused by the gradient of the absorption peaks, that is, the gradient of the refractive index. The retrieval time of the echoed photons observed in this experiment (the appearance time of the peaks on the right) is the sum of the delay time owing to the slow light effect and storage time in the quantum memory.

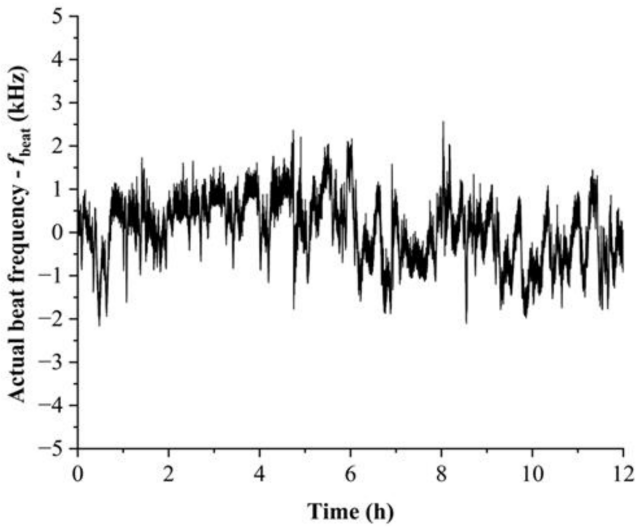

FIG. 4. Result of relative frequency stabilization. In a 12-h measurement, the relative frequency drift is maintained below 5 kHz.

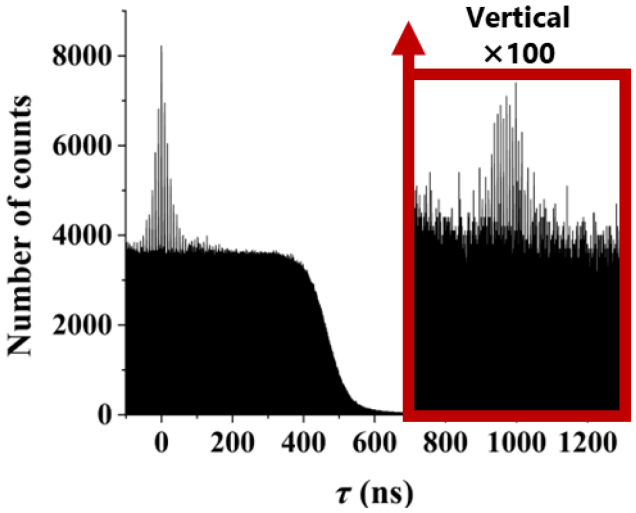

FIG. 6. Results of a 10-km-optical-fiber transmission experiment. This experiment is performed with a TIA time resolution of 0.128 ns. Peaks derived from the retrieved photon from the quantum memory can be observed in the noise-cut region (right side of the figure).

We also use this system to extract a few frequency modes by replacing the long optical fiber with a 5-m fiber. Figure 7 depicts the situation when the five- or one-frequency mode is generated. The vertical axis represents the SNR, and the time on the horizontal axis is the same as that in Fig. 6. The measurement times are 12 and 42 h, respectively, and the time resolution of the TIA is set at 0.128 ns. These results indicate that the SNR at each peak is 0.87 and 0.17, respectively. Because a frequency-multiplexed two-photon source is utilized in this study, a large frequency multiplicity leads to a high SNR, as the probability of two pairs generating simultaneously in the same frequency mode decreases. Therefore, the pump power of the TPC can be increased when compared with the one-frequency-mode case.

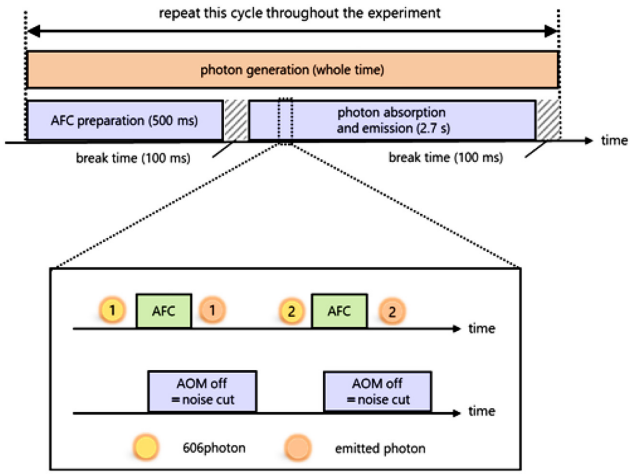

FIG. 5. Timescale of the experiment. Photons are constantly generated from the TPC. Quantum memory experiment is divided into the time to prepare the AFC and the time to transmit photons. During the photon transmission time, the AOM shutter reduces noise from the cavity and wavelength-conversion pump lights.

III. DISCUSSION

In this study, we generate 1–25 wavelength channels in our quantum memory and demonstrate 10-km-optical-fiber transmission of the frequency-multiplexed TPC. In actual quantum communication, by creating a situation in which

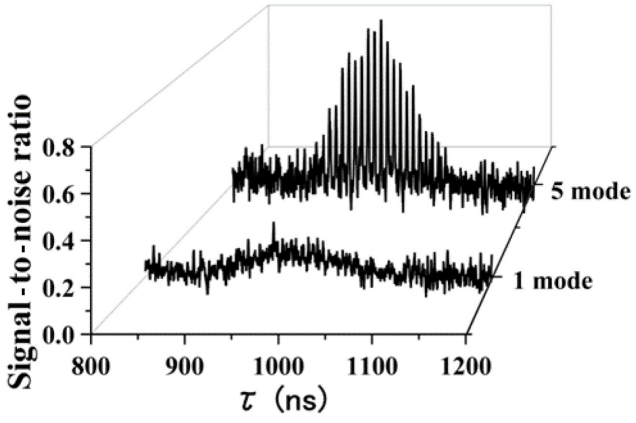

FIG. 7. Experimental results pertaining to the one mode and five mode. Time resolution of the TIA is 0.128 ns, and the adjacent average is considered for 10 bins (=1.28 ns). These data are normalized by the noise floor.

each wavelength channel can be separately detected, indistinguishability [23,38] can be obtained in the BSM and an improvement in the quantum entanglement generation rate between quantum memories can be achieved with the advantage of frequency multiplexing. It will be necessary to acquire the ability to identify each wavelength channel and perform entanglement swapping. Previous studies investigated quantum interference between multiple wavelengths, including wavelength-to-spatial-mode switching [38] and wavelength-to-time conversion to discriminate by varying the AFC retrieval time for each channel [39]. This indicates that wavelength-division-multiplexed entanglement swapping for quantum repeaters is possible. For a two-photon source located in a memory-equipped repeater node, the photon generates a heralding signal for the entanglement swapping operation through optical BSM at the midpoint of the optical fiber transmission [23,40], where the two abovementioned methods can be applied. In this study, it is assumed that entangled two-photon generation is performed at a midpoint separated from the quantum memory [41,42] and that the photons are transmitted to each quantum memory on both sides, which requires wavelength distinguishability in the quantum memory. When employing AFC quantum memories, as in this study, the AFC's peak spacing of 25 channels can be changed to identify the channels using their retrieval time [43]. It is possible to increase the number of frequency-multiplexing channels to approximately 50, utilizing the inhomogeneous broadening width of Pr:YSO. This would increase the excitation power of the entangled photon source, as described in Sec. II, which would increase the SNR and improve the resulting quantum entanglement fidelity.

In this study, we successfully measure two-photon correlation after fiber transmission over 10 km. However, the small signal-to-noise ratio is an obstacle in the demonstration of quantumness, including high-fidelity entanglement. Future improvements will include the use of two-photon sources with higher spectral brightness, which can lead to a higher signal-to-noise ratio, such as a nondegenerate two-photon source, which can narrow the two-photon-generated cluster width by 2 orders of magnitude or more [26,44] and, thereby, improve the rate of signal photons that couple with the AFC.

The photon source, quantum memory, and wavelength-conversion system demonstrated in this study can be stably coupled for long periods of time using a frequency-stabilization system. The present coupling system of remote quantum devices through the frequency-stabilization system will also enable a connection to other physical systems. If the system is to be connected to other quantum memory systems [15,16,19] as an end node of the quantum internet, the propagating photon must acquire indistinguishability [20] by wavelength conversion and frequency stabilization. This is because a quantum repeater through BSMs among hybrid physical systems becomes possible only when indistinguishability is achieved. Moreover, because indistinguishability is expected to be mediated by wavelength conversion [20], the method proposed in our study can be used.

Here, an optical fiber quantum repeater is assumed because a telecommunication-wavelength quantum photon source is used, but the developed coupled system can also be used in a hybrid quantum internet, where a satellite-based quantum repeater is combined. This is because wavelength conversion is necessary to connect the photon wavelengths used for satellite-to-ground quantum communication with the ground-side quantum internet nodes. In terms of feasibility, GPS combs can potentially be used as a frequency reference for the frequency stabilization of quantum devices onboard satellites for quantum repeaters [6–8].

There are variations in entanglement generation between the elementary links towards quantum repeaters. In the midpoint source scheme [41,42], two entangled photons of a telecommunication wavelength are sent to repeater nodes on the left and right, as in this study [Fig. 8(a)]. At these points, they are wavelength converted to quantum memory wavelengths and absorbed and stored in quantum memories. This method enables entanglement sharing at a higher rate when compared with conventional methods [41]. However, the drawback of this method is that it cannot generate heralding signals when using absorptive quantum memories. Therefore, a method such as nondestructive photon-arrival detection [42,45] is required to be implemented just before the memory, which is technically difficult at present. In contrast, in the meet-in-the-middle scheme [Fig. 8(b)], the entangled photon source is installed in the same node as the quantum memory. In this case, a single photon from the generated two-photon (degenerate telecommunication wavelength, as used here) is converted into the quantum memory wavelength on the spot and is absorbed and stored

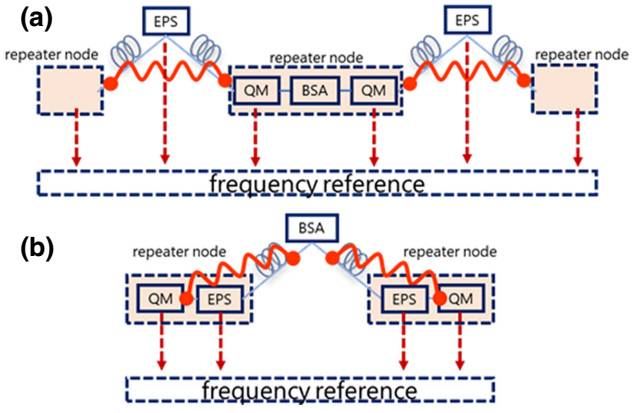

FIG. 8. Available schemes for entanglement generation: (a) midpoint source, (b) meet in the middle. EPS: entangled-photon source, BSA: Bell state analyzer.

in the quantum memory. The other photon is measured at an intermediate station through an optical fiber to generate an entanglement-heralding signal in the elementary link [46]. Thus, this scheme overcomes the drawback that an absorptive quantum memory itself cannot generate heralding signals. As the wavelength-conversion efficiency of photons stored in a quantum memory can be more than 50%, there is no significant loss caused by this. It is also possible to generate one of the two photons directly at the quantum memory wavelength, in which case, wavelength conversion itself can be avoided.

In addition, the present wavelength conversion can also be incorporated into the meet-in-the-middle case. As studied in the frequency identification among frequency-multiplexed system [43], Pr:YSO can be responsible for the frequency identification for the incoming telecom photons at the intermediate station. Therefore, the present efficient wavelength-conversion system and the frequency-identification system utilizing the AFC generated in Pr:YSO at the intermediate station will enable frequency-multiplexed BSM.

To connect multiple repeater nodes, it is necessary to transmit a telecommunication-wavelength laser between nodes in the case of an optical fiber. Because the loss of the telecommunication-wavelength signal is 0.2 dB/km, assuming the typical distance of repeater nodes is 50 km, the loss is 10 dB, which means that the laser can be transmitted to multiple nodes comprising the quantum internet without any problem. In addition, because the stabilizing laser is classical light, it is relatively easy to transmit over long distances by inserting a fiber amplifier in the middle of the transmission. For example, it is possible to send a 1514-nm laser that is absolute frequency locked to a GPS optical frequency comb to a remote node through an optical fiber. The 1212-nm laser, which is a fundamental laser of the quantum memory control laser, can be frequency stabilized under the same reference because it can be used as a reference for another optical comb installed within that node.

In this manner, our optical frequency-comb-based photon-source–quantum memory coupling system can be deployed globally with a unified frequency standard.

Here, we succeed in coupling photons generated by a telecommunication-wavelength TPC to a frequency-multiplexed quantum memory through wavelength conversion after long-optical-fiber transmission. The developed system is promising in the context of the future quantum repeater architecture. The next step will be to demonstrate a frequency-multiplexed quantum repeater and expand it to multiple repeater nodes using the developed system.

ACKNOWLEDGMENTS

We thank Qiang Zhang, Kazumichi Yoshii, Ippei Nakamura, Shuhei Tamura, Tomoki Tsuno, Takuto Miyashita, Yuma Goji, and Ryo Onozawa for their support in the experiments. Tomoyuki Horikiri also acknowledges members of the Quantum Internet Task Force, which is a research consortium set with the task of realizing the quantum internet, for comprehensive and interdisciplinary discussions of the quantum internet. We acknowledge funding from the SECOM foundation, JST PRESTO (Grant No. JPMJPR1769), JST START (Grant No. ST292008BN), JSPS KAKENHI (Grant No. JP20H02652), NEDO (Grant No. JPNP14012), and JST Moonshot R&D (Grant No. JPMJMS226C).

[1] A. Broadbent, J. Fitzsimons, and E. Kashefi, in Proceedings of the 50th Annual IEEE Symposium on Foundations of Computer Science (FOCS) (2009), pp. 517–526.

[2] P. Kómár, E. M. Kessler, M. Bishof, L. Jiang, A. S. Sørensen, J. Ye, and M. D. Lukin, A quantum network of clocks, Nat. Phys. **10**, 582 (2014).

[3] D. Gottesman, T. Jennewein, and S. Croke, Longer-Baseline Telescopes Using Quantum Repeaters, Phys. Rev. Lett. **109**, 070503 (2012).

[4] J. Yin, Y. Cao, Y.-H. Li, S.-K. Liao, L. Zhang, J.-G. Ren, W.-Q. Cai, W.-Y. Liu, B. Li, H. Dai, *et al.*, Satellite-based entanglement distribution over 1200 kilometers, Science **356**, 1140 (2017).

[5] M. Gündoğan, T. Jennewein, F. K. Asadi, E. D. Ros, E. Sağlamyürek, D. Oblak, T. Vogl, D. Rieländer, J. Sidhu, S. Grandi, *et al.*, "Topical white paper: A case for quantum memories in space." *Preprint at arXiv* https://arxiv.org/abs/2111.09595 (2021).

[6] C. Liorni, H. Kampermann, and D. Bruß, Quantum repeaters in space, New J. Phys. **23**, 053021 (2021).

[7] M. Gündoğan, J. S. Sidhu, V. Henderson, L. Mazzarella, J. Wolters, D. K. L. Oi, and M. Krutzik, Proposal for space-borne quantum memories for global quantum networking, npj Quantum Inf. **7**, 128 (2021).

[8] K. Boone, J.-P. Bourgoin, E. Meyer-Scott, K. Heshami, T. Jennewein, and C. Simon, Entanglement over global distances via quantum repeaters with satellite links, Phys. Rev. A **91**, 052325 (2015).

[9] S. Langenfeld, P. Thomas, O. Morin, and G. Rempe, Quantum Repeater Node Demonstrating Unconditionally Secure Key Distribution, Phys. Rev. Lett. **126**, 230506 (2021).

[10] S. Welte, B. Hacker, S. Daiss, S. Ritter, and G. Rempe, Photon-Mediated Quantum Gate between Two Neutral Atoms in an Optical Cavity, Phys. Rev. X **8**, 011018 (2018).

[11] L. J. Stephenson, D. P. Nadlinger, B. C. Nichol, S. An, P. Drmota, T. G. Ballance, K. Thirumalai, J. F. Goodwin, D. M. Lucas, and C. J. Ballance, High-Rate, High-Fidelity Entanglement of Qubits across an Elementary Quantum Network, Phys. Rev. Lett. **124**, 110501 (2020).

[12] M. K. Bhaskar, R. Riedinger, B. Machielse, D. S. Levonian, C. T. Nguyen, E. N. Knall, H. Park, D. Englund, M. Lončar, D. D. Sukachev, *et al.*, Experimental demonstration of memory-enhanced quantum communication, Nature **580**, 60 (2020).

[13] D. Lago-Rivera, S. Grandi, J. V. Rakonjac, A. Seri, and H. de Riedmatten, Telecom-heralded entanglement

between multimode solid-state quantum memories, Nature **594**, 37 (2021).

[14] X. Liu, J. Hu, Z. F. Li, X. Li, P. Y. Li, P. J. Liang, Z. Q. Zhou, C. F. Li, and G. C. Guo, Heralded entanglement distribution between two absorptive quantum memories, Nature **594**, 41 (2021).

[15] Y. Yu, F. Ma, X.-Y. Luo, B. Jing, P.-F. Sun, R.-Z. Fang, C.-W. Yang, H. Liu, M.-Y. Zheng, X.-P. Xie, *et al.*, Entanglement of two quantum memories via fibres over dozens of kilometres, Nature **578**, 240 (2020).

[16] M. Pompili, S. L. N. Hermans, S. Baier, H. K. C. Beukers, P. C. Humphreys, R. N. Schouten, R. F. L. Vermenlen, M. J. Tiggelman, L. Dos Santos Martings, B. Dirkse, *et al.*, Realization of a multinode quantum network of remote solid-state qubits, Science **372**, 259 (2021).

[17] X.-Y. Luo, Y. Yu, J.-L. Liu, M.-Y. Zheng, C.-Y. Wang, B. Wang, J. Li, X. Jiang, X.-P. Xie, Q. Zhang *et al.*, "Entangling metropolitan-distance separated quantum memories," Preprint at arXiv https://arxiv.org/abs/2201.11953 (2022).

[18] T. v. Leent, M. Bock, F. Fertig, R. Garthoff, S. Eppelt, Y. Zhou, P. Malik, M. Seubert, T. Bauer, W. Rosenfeld, *et al.*, Entangling single atoms over 33 km telecom fibre, Nature **607**, 69 (2022).

[19] T. Walker, K. Miyanishi, R. Ikuta, H. Takahashi, S. V. Kashanian, Y. Tsujimoto, K. Hayasaka, T. Yamamoto, N. Imoto, and M. Keller, Long-Distance Single Photon Transmission from a Trapped Ion via Quantum Frequency Conversion, Phys. Rev. Lett. **120**, 203601 (2018).

[20] L. Yu, C. M. Natarajan, T. Horikiri, C. Langrock, J. S. Pelc, M. G. Tanner, E. Abe, S. Maier, C. Schneider, S. Höfling, *et al.*, Two-photon interference at telecom wavelengths for time-bin-encoded single photons from quantum-dot spin qubits, Nat. Commun. **6**, 8955 (2015).

[21] M. Afzelius, C. Simon, H. De Riedmatten, and N. Gisin, Multimode quantum memory based on atomic frequency combs, Phys. Rev. A **79**, 052329 (2009).

[22] M. Nilsson, L. Rippe, S. Kröll, R. Klieber, and D. Suter, Hole-burning techniques for isolation and study of individual hyperfine transitions in inhomogeneously broadened solids demonstrated in $Pr^{3+} : Y_2SiO_5$, Phys. Rev. B **70**, 214116 (2004).

[23] N. Sinclair, E. Saglamyurek, H. Mallahzadeh, J. A. Slater, M. George, R. Ricken, M. P. Hedges, D. Oblak, C. Simon, W. Sohler, *et al.*, Spectral Multiplexing for Scalable Quantum Photonics Using an Atomic Frequency Comb Quantum Memory and Feed-Forward Control, Phys. Rev. Lett. **113**, 053603 (2014).

[24] K. Mannami, T. Kondo, T. Tsuno, T. Miyashita, D. Yoshida, K. Ito, K. Niizeki, I. Nakamura, F. Hong, and T. Horikiri, Coupling of a quantum memory and telecommunication wavelength photons for high-rate entanglement distribution in quantum repeaters, Opt. Express **29**, 41522 (2021).

[25] K. Niizeki, D. Yoshida, K. Ito, I. Nakamura, N. Takei, K. Okamura, M. Zheng, X. Xie, and T. Horikiri, Two-photon comb with wavelength conversion and 20-km distribution for quantum communication, Commun. Phys. **3**, 138 (2020).

[26] J. Fekete, D. Rieländer, M. Cristiani, and H. de Riedmatten, Ultranarrow-Band Photon-Pair Source Compatible with Solid State Quantum Memories and Telecommunication Networks, Phys. Rev. Lett. **110**, 220502 (2013).

[27] A. Seri, D. Lago-Rivera, A. Lenhard, G. Corrielli, R. Osellame, M. Mazzera, and H. de Riedmatten, Quantum Storage of Frequency-Multiplexed Heralded Single Photons, Phys. Rev. Lett. **123**, 080502 (2019).

[28] T. Miyashita, T. Kondo, K. Ikeda, K. Yoshii, F. Hong, and T. Horikiri, Offset-locking-based frequency stabilization of external cavity diode lasers for long-distance quantum communication, Jpn. J. Appl. Phys. **60**, 122001 (2021).

[29] U. Schünemann, H. Engler, R. Grimm, M. Weidemüller, and M. Zielonkowski, Simple scheme for tunable frequency offset locking of two lasers, Rev. Sci. Instrum. **70**, 242 (1999).

[30] Y. Hisai, K. Ikeda, H. Sakagami, T. Horikiri, T. Kobayashi, K. Yoshii, and F. L. Hong, Evaluation of laser frequency offset locking using an electrical delay line, Appl. Opt. **57**, 5628 (2018).

[31] S. Tamura, K. Ikeda, K. Okamura, K. Yoshii, F. Hong, T. Horikiri, and H. Kosaka, Two-step frequency conversion for connecting distant quantum memories by transmission through an optical fiber, Jpn. J. Appl. Phys. **57**, 062801 (2018).

[32] J. S. Pelc, L. Ma, C. R. Phillips, Q. Zhang, C. Langrock, O. Slattery, X. Tang, and M. M. Fejer, Long-wavelength-pumped upconversion single-photon detector at 1550 nm: Performance and noise analysis, Opt. Express **19**, 21445 (2011).

[33] P. C. Strassmann, A. Martin, N. Gisin, and M. Afzelius, Spectral noise in frequency conversion from the visible to the telecommunication C-band, Opt. Express **27**, 14298 (2019).

[34] N. Maring, K. Kutluer, J. Cohen, M. Cristiani, M. Mazzera, P. M. Ledingham, and H. d. Riedmatten, Storage of up-converted telecom photons in a doped crystal, New J. Phys. **16**, 113021 (2014).

[35] J. S. Pelc, C. Langrock, Q. Zhang, and M. M. Fejer, Influence of domain disorder on parametric noise in quasi-phase-matched quantum frequency converters, Opt. Lett. **35**, 2804 (2010).

[36] A. Walther, A. Amari, S. Kröll, and A. Kalachev, Experimental superradiance and slow-light effects for quantum memories, Phys. Rev. A **80**, 012317 (2009).

[37] P. W. Milonni, Controlling the speed of light pulses, J. Phys. B **35**, R31 (2002).

[38] O. Pietx-Casas, G. C. do Amaral, T. Chakraborty, R. Berrevoets, T. Middelburg, J. A. Slater, W. Tittel, "Spectrally multiplexed Hong-Ou-Mandel interference," *Preprint at arXiv* https://arxiv.org/abs/2111.13610 (2021).

[39] E. Saglamyurek, N. Sinclair, J. A. Slater, K. Heshami, D. Oblak, and W. Tittel, An integrated processor for photonic quantum states using a broadband light–matter interface, New J. Phys. **16**, 065019 (2014).

[40] C. Simon, H. de Riedmatten, M. Afzelius, N. Sangouard, H. Zbinden, and N. Gisin, Quantum Repeaters with Photon Pair Sources and Multimode Memories, Phys. Rev. Lett. **98**, 190503 (2007).

[41] C. Jones, D. Kim, M. T. Rakher, P. G. Kwiat, and T. D. Ladd, Design and analysis of communication protocols

for quantum repeater networks, New J. Phys. **18**, 083015 (2016).

[42] D. Yoshida, K. Niizeki, S. Tamura, and T. Horikiri, Entanglement distribution between quantum repeater nodes with an absorptive type memory, Int. J. Quantum Inf. **18**, 2050026 (2020).

[43] D. Yoshida, M. Ichihara, T. Kondo, F. Hong, and T. Horikiri, Single-shot high-resolution identification of discrete frequency modes of single-photon-level optical pulses, Phys. Rev. **A106**, 052602 (2022).

[44] R. Onozawa, D. Yoshida, K. Niizeki, and T. Horikiri, Cavity-enhanced two-photon source emitting narrow linewidth telecommunication wavelength photons for improved quantum memory-coupling efficiency enabling long-distance quantum communications, Jpn. J. Appl. Phys. **61**, 102008 (2022).

[45] N. Sinclair, K. Heshami, C. Deshmukh, D. Oblak, C. Simon, and W. Tittel, Proposal and proof-of-principle demonstration of non-destructive detection of photonic qubits using a Tm : $LiNbO_3$ waveguide, Nat. Commun. **7**, 13454 (2016).

[46] L.-M. Duan, M. D. Lukin, J. I. Cirac, and P. Zoller, Long-distance quantum communication with atomic ensembles and linear optics, Nature **414**, 413 (2001).